ELSEVIER

Desalination 167 (2004) 361–368

DESALINATION

www.elsevier.com/locate/desal

Contribution to the comprehension of the calcium ions transfer phenomena through a nanofiltration spiral wound membrane

T. Chaabane[a*], S. Taha[b], N. Ameraoui[a], G. Dorange[b], R. Maachi[a]

[a]*Laboratoire de Génie de la Réaction Chimique, FGM and GP, USTHB, BP 32 El-Alia 16111, Algiers, Algeria*
Tel. +213 (21) 246971; Fax +213 (21) 246971; e-mail: tfkchaabane@yahoo.fr
[b]*Laboratoire de Chimie des Eaux et de l'Environnement, ENSCR, Avenue du Général Leclerc, 35700 Rennes, France*
Tel.+33 (2) 23238015; Fax +33 (2) 23238199; e-mail: samir.taha@ensc-rennes.fr

Received 6 February 2004; accepted 16 February 2004

Abstract

A mathematical model is proposed to predict the transfer mechanism of calcium salts through a nanofiltration membrane. The model is a combination of Nernst-Planck and film theory equations and it is characterized by three transport parameters: solute permeability P_s, reflection coefficient σ and film thickness δ. In the present work, the influence of including concentration polarization phenomena on salt rejection is studied and the thickness of the boundary layer formed at the feed side adjacent to the membrane, δ, is estimated. Model results were shown to be in good agreement with experimental data at various operating conditions of pressure, temperature and initial concentration. The results show that including concentration, polarization has not a great effect on salt rejection for the present operating conditions. Estimated thickness of boundary layer formed near the membrane surface was too small and ranged between 10^{-13} and 10^{-12} m. In later work, we plan to perform some experiments at different operating conditions as higher initial concentration of calcium salts or lower tangential flow to bring the system in polarization concentration and then to apply, verify and validate the model proposed.

Keywords: Polarisation concentration; Calcium rejection; Nanofiltration; Modeling

1. Introduction

One of the innovative technologies that are gaining broad application in potable water treatment is the membrane process. These processes have been utilized for desalination of seawater and salt water for several decades, and since the early 80's for the removal of suspended and dissolved constituents in surface and ground-

*Corresponding author

Presented at the EuroMed 2004 conference on Desalination Strategies in South Mediterranean Countries: Cooperation between Mediterranean Countries of Europe and the Southern Rim of the Mediterranean. Sponsored by the European Desalination Society and Office National de l'Eau Potable, Marrakech, Morocco, 30 May–2 June, 2004.

0011-9164/04/$– See front matter

doi;10.1016/j.desal.2004.06.147

water. Efficiency, reliability and relatively low treatment costs resulted in mass application of membrane filtration systems.

Nanofiltration (NF) is the most recently developed pressure-driven membrane process for liquid-phase separation [1]. It has found wide applications in many industries such as separation of no-sucrose compounds in the sugar industry [2], recovery of caustic cleaning-in-place solutions in the dairy industry [3], removal of heavy metals in soil operations [4], separation of surfactant in the detergent industry [5], recovery of dye from textile effluent [6], treatment of paper mill process water [7] and removal of colour from industrial waste water [8].

The properties of the NF membranes lie between those of non-porous reverse osmosis (RO) membranes (where transport is governed by a solution-diffusion mechanism) and porous ultrafiltration (UF) membranes where separation is usually assumed to be due to size exclusion and, in some cases, charge effects [9].

Their separation mechanisms involve both steric (sieving) effects and electrical (Donnan) effects. This combination allows NF membranes to be effective for a range of separations of mixtures of small organic solutes (either neutral or charged) and salts [10]. Various models have been proposed in modelling the rejection mechanisms of charged (ionic) species by NF membranes. Most of these models were based on the Nernst-Planck equation.

The aim of the present work is to propose a model for predicting the transfer mechanism of divalent ions through NF membranes by including the concentration polarization phenomena and to study its influence on the salt rejection. This model is a combination of Nernst-Planck and film theory equations and it is characterized by three transfer parameters which are solute permeability *Ps*, reflection coefficient σ and film thickness δ.

In this paper, mathematical formulation of the model is reported. Calcium salt rejections are estimated and compared to experimental results for a binary system. A comparison between results with and without concentration polarization phenomena is made and the thickness of the boundary layer on the feed side adjacent to the membrane δ, is also estimated.

2. Theoretical aspect

Extended Nernst-Planck equation is the fundamental relationship governing the transport of ionic species through membrane pores. It is now well understood that rejection of ions by membrane pores is a manifestation of the equilibrium partitioning behaviour of the ions at the pore-solution interface and the ionic fluxes generated through convective, diffusive and electrostatic potential driven migration forces [11].

By considering the motion of compounds unidirectional through the membrane and assuming dilute solutions, the transport equation for a specie *i* can be written as [12]:

$$J_i = -P_i^* \left[\frac{dC_i}{dx} + \frac{FZ_iC_i}{\Re T} \frac{d\Psi}{dx} \right] + J_v C_i (1-\sigma_i) \quad (1)$$

For a binary system, the permeate flow of each specie is:

$$J_1 = -P_1^* \left[\frac{dC_1}{dx} + \frac{FZ_1C_1}{\Re T} \frac{d\Psi}{dx} \right] + J_v C_1 (1-\sigma_1) \quad (2)$$

$$J_2 = -P_2^* \left[\frac{dC_2}{dx} + \frac{FZ_2C_2}{\Re T} \frac{d\Psi}{dx} \right] + J_v C_2 (1-\sigma_2) \quad (3)$$

By rearranging Eqs. (2) and (3) together with electroneutrality conditions:

$$\sum\nolimits_i Z_i C_i = 0 \quad (4)$$

$$\sum\nolimits_i Z_i J_i = 0 \quad (5)$$

Eq. (1) becomes:

$$J_1 = -P \frac{dC_1}{dx} + J_v C_1 (1-\sigma_1) \quad (6)$$

where:

$$P=\frac{\left(1-\frac{Z_2}{Z_1}\right)}{\left(1-\frac{Z_2P_2^*}{Z_1P_1^*}\right)};\ \sigma=\left[\frac{\left(\sigma_2-\frac{Z_2P_2^*}{Z_1P_1^*}\sigma_1\right)}{\left(1-\frac{Z_2P_2^*}{Z_1P_1^*}\right)}\right] \quad (7)$$

P and σ are constant characteristics of each salt. They depend on the permeability of each ion, and on its charge density (further details are given in a previous work [12]).

This differential equation (Eq. (6)) is the so-called Kedem & Spiegler equation, in which the terms on the right hand side represent transport due to diffusion (corresponding to the migration of the ion due to the concentration gradient effect), and convection (related to ion transport by the solvent) respectively.

Eq. (6) is integrated over the membrane thickness ($0<x<\Delta x$) using the following boundary conditions:

$$C_1 = C_{m_1}^* \text{ at } x=0 \quad (8a)$$

$$C_1 = C_{P_1}^* \text{ at } x=\Delta x \quad (8b)$$

$$\text{and } J_1 = C_{P_1}^* . J_v \quad (9)$$

The solution is:

$$C_{m1}=\left(1-\frac{\sigma}{\exp[(1-\sigma)J_v/P_s]}\right)\frac{C_{P_1}^*}{1-\sigma} \quad (10)$$

where: $P_s=\frac{P}{\Delta x}$

According to Donnan equations [13], the concentration of ion 1 at the feed and permeate interfaces can be written as follows:

$$C_{m_1}^* = C_{m_1}\exp\left(-\frac{z_1F\Delta\Psi_D}{\Re T}\right) \quad (11)$$

$$C_{P_1}^* = C_{P_1}\exp\left(-\frac{z_1F\Delta\Psi_D}{\Re T}\right) \quad (12)$$

and so, Eq. (10) becomes:

$$C_{m_1}=\left(1-\sigma.\exp\left[-\frac{(1-\sigma)J_v}{P_s}\right]\right)\frac{C_{P_1}}{1-\sigma} \quad (13)$$

2.1. Neglecting concentration polarization

As the system was operated in a closed loop, the concentration of ion 1 at the interface of the membrane can be taken equal to that in the feed solution. i.e.; $C_{m_1} = C_{0_1}$ (see Fig. 1.).

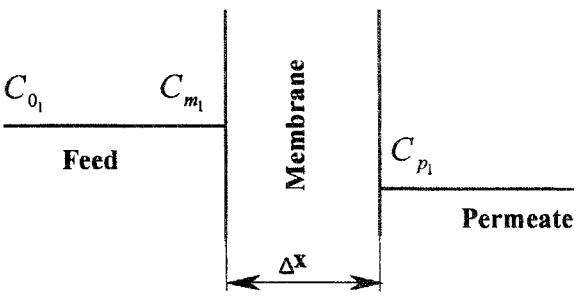

Fig. 1. Concentration profile in the membrane-solution system.

Eq. (13) becomes:

$$C_{0_1}=\left(1-\sigma.\exp\left[-\frac{(1-\sigma)J_v}{P_s}\right]\right)\frac{C_{P_1}}{1-\sigma} \quad (14)$$

and the retention of ion 1 is given by:

$$R=1-\frac{1-\sigma}{1-\sigma.\exp\left[-\frac{(1-\sigma)J_v}{P_s}\right]} \quad (15)$$

We note that for the binary solutions, $R_{salt}=R_{cation}=R_{anion}$. This expression is similar to those found in the literature [12].

2.2. Considering concentration polarization

In this case, predicting the solute rejection requires a coupled solution of two transport models: the first one describes the transfer mechanism in the concentration polarization boundary layer near the membrane at the feed interface based on the film theory, while the second describes the transport in the membrane pores using the extended Nernst-Planck equation. The transport phenomenon is described in Fig. 2.

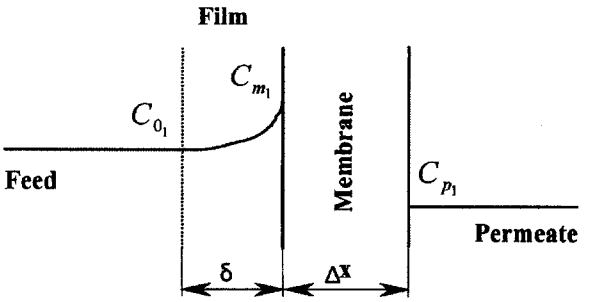

Fig. 2. Concentration profile in the film-membrane system.

Concentration polarisation close to the membrane surface is assumed to occur within a boundary film of thickness δ, which is dependent on the mass transfer characteristics of the system [10].

According to the film theory [13], the concentration polarization is given by:

$$J_1 = -D_1 \frac{dC_1}{dx} + C_1 J_v \tag{16}$$

Integration of Eq. (16) over the thickness of the boundary layer δ gives:

$$C_{m_1} = C_{p_1} - (C_{p_1} - C_{0_1}) \exp\left(\frac{\delta}{D_1} J_v\right) \tag{17}$$

Eq. (17) is then equal to Eq. (13), and so:

$$\frac{C_{p_1}}{C_{0_1}} = \frac{1}{1 + \frac{\sigma}{1-\sigma}\left[\exp\left(-J_v.\frac{\delta}{D_1}\right) - \exp\left(-\frac{(1-\sigma)J_v}{P_s} - \frac{J_v.\delta}{D_1}\right)\right]} \tag{18}$$

The rejection of ion 1 can then be written as:

$$R = 1 - \frac{1}{1 + \frac{\sigma}{1-\sigma}\left[\exp\left(-J_v.\frac{\delta}{D_1}\right) - \exp\left(-\frac{(1-\sigma)J_v}{P_s} - \frac{J_v.\delta}{D_1}\right)\right]} \tag{19}$$

3. Results and discussion

3.1. Model parameters

Eqs. (15) and (19) are used for the prediction of salt rejection, then, to estimate model parameters without and with concentration polarization phenomena respectively. A computer program in Fortran Power Station language is performed to find the smallest value of error (ε) while varying the thickness of the boundary layer δ and the two transport parameters σ and P_s over appropriate intervals. Results are shown in Tables 1 and 2.

We note that ε is given by:

$$\varepsilon = \sum_N \left| R_{th} - R_{\exp} \right|^2$$

Table 1
Model parameters without concentration polarization

Solution	Concentration, mmol. L^{-1}	Transport parameters, with polarization concentration		
		σ	$P_s 10^6$ m.s^{-1}	ε
$Ca(CH_3COO)_2$	0.5	0.3634	3.073	0.0167
	1.0	0.4089	0.686	0.0193
	1.5	0.4650	0.985	0.0123
$Ca(NO_3)_2$	0.5	0.2003	1.061	0.0185
	1.0	0.1839	2.226	0.0351
	1.5	0.1673	2.197	0.0467
$CaCl_2$	0.5	0.2186	1.119	0.0171
	1.0	0.1474	0.889	0.0090
	1.5	0.1592	0.919	0.0186

Table 2
Model parameters with concentration polarization

Solution	Concentration mmol. L^{-1}	Transport parameters, without polarization concentration		
		σ	$P_s 10^6$ m.s^{-1}	ε
$Ca(CH_3COO)_2$	0.5	0.3630	3.069	0.0163
	1.0	0.4090	0.686	0.0192
	1.5	0.4580	0.959	0.0123
$Ca(NO_3)_2$	0.5	0.2000	1.058	0.0184
	1.0	0.1840	2.228	0.0350
	1.5	0.1600	2.072	0.0323
$CaCl_2$	0.5	0.2185	1.119	0.0168
	1.0	0.1473	0.888	0.0087
	1.5	0.1591	0.918	0.0183

3.2. Salt rejection with and without including concentration polarization

Estimated model parameters σ and P_s are used to calculate theoretical salt rejection of $Ca(CH_3COO)_2$, $Ca(NO_3)_2$ and $CaCl_2$ at different concentrations. In Figs. 3, 4 and 5, a comparison is shown between model predictions and experimental results for calcium salts with and without concentration polarization.

Curves show an agreement between model and experimental rejection data for all salts as the diagram of parity confirms (Fig. 6).

They also show that including concentration polarization phenomena does not have a great effect on salts rejection: theoretical and experimental curves are almost superimposed for all salts, Fig. 7. This is confirmed by calculated model parameter values, with and without concentration polarization, which are very close (Tables 1 and 2).

This effect can be explained by both low feed salt concentration, which was in the order of magnitude of mmol/L, and the effect of permitting tangential cross flow to destroy the con-

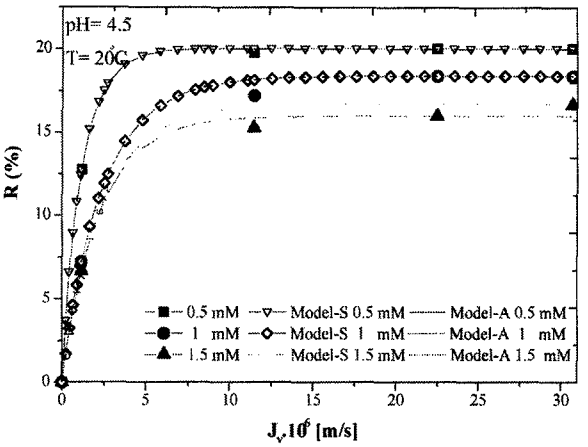

Fig. 3. Comparison between calculated and experimental rejections with and without concentration polarization phenomena for $Ca(NO_3)_2$.

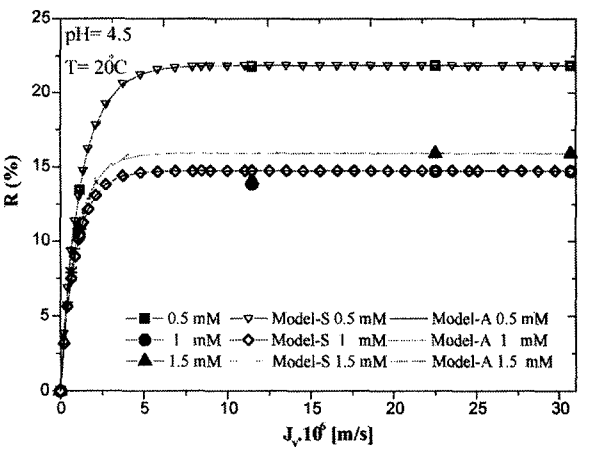

Fig. 4. Comparison between calculated and experimental rejections with and without concentration polarization phenomena for $Ca(CH_3COO)_2$.

centration polarization boundary layer formed at the feed side adjacent to the membrane.

The estimated boundary layer thickness, δ, is too small and ranges between 10^{-13} and 10^{-12} m for all calcium salts where some examples are given in Table 3.

Nevertheless, we note a slight amelioration when including concentration polarization if comparing calculated error values reported in Tables 1 and 2 respectively.

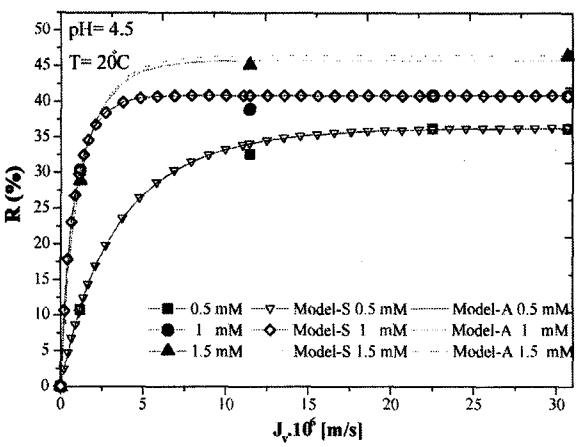

Fig. 5. Comparison between calculated and experimental rejections with and without concentration polarization phenomena for $CaCl_2$.

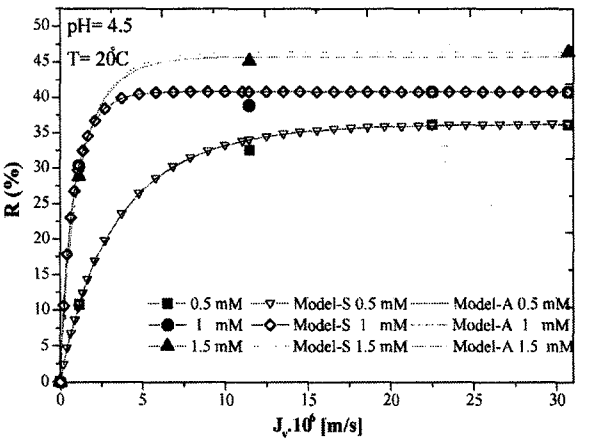

Fig. 6. Diagram of parity for calcium salts.

4. Conclusion

A coupled model, based on Nernst-Planck and film theory equations, was proposed to predict the transfer mechanism of divalent ions through nanofiltration membranes. The model is characterized by three transport parameters: solute permeability P_s, reflection coefficient σ and film thickness δ. The influence of concentration polarization phenomena on calcium salt rejection was studied. Model results were shown to be in good agreement with experimental data and show that including concentration polariza-

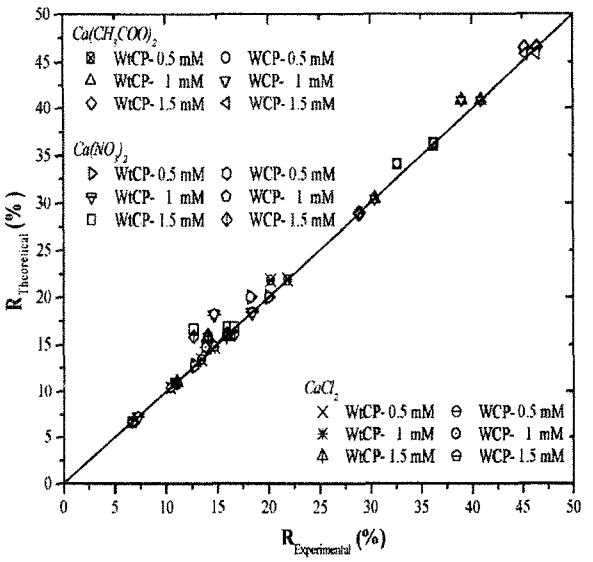

Fig. 7. Theoretical and experimental curves almost superimposed for all salts.

Table 3
Estimated boundary layer thickness, δ, at 1.5 mmol/L

Salt	Concentration mmol. L^{-1}	δ. 10^{-13} m
$Ca(NO_3)_2$	1.5	5.5
$Ca(CH_3COO)_2$	1.5	9
$CaCl_2$	1.5	15

tion has not a great effect on salt rejection for the present operating conditions. Estimated thickness of boundary layer formed near the membrane surface was too small and ranged between 10^{-13} and 10^{-11} m.

5. Symbols

C_i — Ion concentration, mol. L^{-1}

C_{m_i} — Ion concentration at the membrane surface, mol. L^{-1}

$C^*_{m_i}$ — Ion concentration in the membrane at the feed interface, mol. L^{-1}

C_{0_i} — Ion concentration in the feed, mol. L^{-1}

C_{p_i} — Ion concentration in the permeate, mol. L^{-1}

$C^*_{p_i}$ — Ion concentration in the membrane at the permeate interface, mol. L^{-1}

D_i — Diffusion coefficient of ion i, $m^2.s^{-1}$

F — Faraday constant, $C.\ mol^{-1}$

J_i — Ion i flux, mol. $m^{-2}.s^{-1}$

J_v — Solvent flux, $m.s^{-1}$

P^*_i — Ion permeability, $m^2.s^{-1}$

P_s — Local solute permeability, $m^2.s^{-1}$

$\Re$ — Universal gas constant, $J,\ K^{-1}.mol^{-1}$

R_i — Ion i rejection, %

T — Absolute temperature, K

Z_i — Ion charge number, dimensionless

z_i — Ion valence number, dimensionless

x — Distance variable, m

Greek letters

δ — Film thickness, m

$\Delta\Psi_D$ — Donnan potential, V

ε — Error

σ — Salt reflection coefficient, dimensionless

σ_i Ion reflection coefficient, dimensionless

Ψ — Electrostatic potential of the system, V

References

[1] W.R. Bowen, J.S. Welfoot and P.M. Williams, Linearized transport model for nanofiltration: Development and assessment, J. AIChE, 48(4) (2002) 760–773.

[2] J. Gyura, Z. Seres, G. Vatai and E.B. Molnar, Separation of non-sucrose compounds from the syrup of sugar-beet processing by ultra- and nanofiltration using polymer membranes, Desalination, 148 (2002) 49–56.

[3] G.G. Guiziou, E. Boyaval and G. Daufin, Nanofiltration for the recovery of caustic cleaning-in-place solutions: robustness towards large varia-

tions of composition, Desalination, 149 (2002) 127–129.
[4] K. Volchek, D. Velicogna, A. Obenauf, A. Somers. B. Wong and A.Y. Tremblay, Novel applications of membrane processes in soil cleanup operations, Desalination, 147 (2002) 123–126.
[5] M. Forstmeier, B. Goers and G. Wozny, UF/NF treatment of rinsing waters in a liquid detergent production plant, Desalination, 149 (2002) 175–177.
[6] A.F. Viero, A.C.R. Mazzarollo, K. Wada and I.C. Tessaro, Removal of hardness and COD from retanning treated effluent by membrane process, Desalination, 149 (2002) 145–149.
[7] M. Manttari, A. Pihlajamaki and M. Nystrom, Comparison of nanofiltration and tight ultrafiltration membranes in the filtration of paper mill process water, Desalination, 149 (2002) 131–136.
[8] M.J.W. Frank, J.B. Westerink and A. Schokker, Re-cycling of industrial wastewater by using a two-step nanofiltration process for the removal of colour, Desalination, 145 (2002) 69–74.
[9] W.R. Bowen and J.S. Welfoot, Modelling the performance of membrane nanofiltration — critical assessment and model development, Chem. Eng. Sci., 57 (2002) 1121–1137.
[10] A.W. Mohammad and M.S. Takriff, Predicting flux and rejection of multicomponent salts mixture in nanofiltration membranes, Desalination, 157 (2003) 105–111.
[11] S. Bhattacharjee, J.C. Chen and M. Elimelech, Coupled model of concentration polarization and pore transport in crossflow nanofiltration, J. AIChE, 47(12) (2001) 2733–2745.
[12] T. Chaabane, S. Taha, J. Cabon, G. Dorange and R. Maachi, Dynamic modelling of mass transfer through a nanofiltration membrane using calcium salt in drinking water, Desalination, 152 (2002) 275–280.
[13] Y. Garba, S. Taha, N. Gondrexon and G. Dorange, Ion transport modelling through nanofiltration membranes, J. Membr. Sci., 160 (1999) 187–200.